JETIR.ORG ISSN: 2349-5162 | ESTD Year : 2014 | Monthly Issue
JOURNAL OF EMERGING TECHNOLOGIES AND INNOVATIVE RESEARCH (JETIR)
An International Scholarly Open Access, Peer-reviewed, Refereed Journal

Study of Operational Efficiency of Different Oil Filters in Heavy-Duty Trucks Using Boltzmann's Theorem

[1]UMAR, Shamsu, [2]AKPUH, Davidson Chioma and [3]Hart Tonye Lawrence

[1,2&3]Federal Polytechnic of Oil and Gas Bonny, Rivers State, Nigeria.

ABSTRACT

The key issue to heavy-duty truck engine's reliability and its durability is the quality of the lubrication system. The primary task of the lubrication system is to provide a continuous supply of filtered oil between two sliding surfaces. By using adequate lubrication oils will reducing friction between moving mechanical parts. Rheological characteristics of lubricating oil directly caused the friction losses due to internal engines mechanisms (piston group, valve train, fuel pump, crankshaft, bearings and seals, etc.). The major focus of this work centers around contamination control in the filtration system of the heavy-duty truck as this dissertation aims at experimentally investigating the operational efficiency of different heavy-duty truck oil filter using Boltzmann theory. In this work, three heavy-duty truck oil filters (labeled A, B and C) were selected, studied and analyzed using the appropriate tests in compliance with SAE (Society of Automobile Engineers) and Boltzmann Theory. The operational efficiency is examined and the reliability of the filter system is assessed systematically by obtaining the filtration performance characteristics such as separation efficiency, filtration performance, discharge, pressure drop etc. The test results show a separation efficiency of 96.3 – 99.9% across the porous media of the filter elements. The results show that the filter A has the highest operational efficiency compared to B and C with a long repair time and cost of repair.
Keywords:

1. INTRODUCTION

Background of the Study

When oil is used in an engine for a long period, undesired metal particles build up in the oil. Rubbing of metal engine parts automatically produces some microscopic metallic particles. Such particles could circulate in the oil and grind against the moving parts, causing erosion and wear. Therefore, to remove those harmful particles, oil filters are used [1-4]

An oil filter with superior filtering ability and holding capacity has the ability to improve engine longevity, increase maintenance intervals and results in substantial savings over the life of the vehicle. Extending an engine's oil drain interval while maintaining the same engine wear, primarily revolves around the durability of the engine oil additive package, the holding capacity and the micron filtering ability of the oil filter [4-7]].

Early internal combustion engines did not use oil filters and, coupled with the poor quality of oil available at the time, vehicles required frequent oil changes. Eventually, the first full-flow oil filtration system was developed. Basically, this arrangement allowed for the oil to flow through the filter before it reached the critical working components inside the engine [8-10].

The vast majority of pressurized lubrication systems found in internal combustion engines incorporate some form of filter bypass to protect the engine from starvation under certain circumstances. A good example is very cold weather. In this situation, if the oil is too thick, it is allowed to bypass the filter. Oil can also bypass the filter when the filter is plugged. Because of these events, oil is sometimes not filtered, even when the engine is fitted with a full-flow oil filter [11-16].

In operation, oil enters the oil filter through a series of small holes on the outer edge of the base flange. The oil is then directed through the filter, eventually making an exit into the engine through the large center hole. Most modern oil filters are equipped with an anti-drainback valve. This is often some form of rubber membrane that covers the perimeter holes in the base flange. The membrane is forced aside as oil enters the filter case. When the engine is not running, the rubber membrane covers the holes. Obviously, the anti-drainback valves maintain oil within the filter. In turn, they prevent engine dry starts (when the engine is started with no oil) [17-20].

Early oil filter designs were based on a replaceable element fitted inside a metal housing. When changing the filter, one removed the housing, discarded the element, cleaned the housing, added a new filter and re-installed the assembly to the engine. By the mid-20th century, spin-on filters gained popularity. There are many types of oil filters available today, and there are likely an equally large number of tests in which various filters are cut apart and diagnosed [20-25].

Aim and Objectives

i. To evaluate filtration characteristics of the filter elements of three different heavy-duty truck oil filter.

ii. To compare the filtration parameters including separation efficiency, filtration performance, volumetric discharge and pressure drop at the filter (media) elements of the different heavy-duty truck oil filter.

iii. To evaluate and compare quality factor of test filters

iv. Simulation and comparison of Boltzmann (diffusive) flow through porous media of the oil filters using MATLAB

v. To determine reliability, maintenance and repair cost of heavy-duty truck oil filter.

Approach to Study

In this work, different heavy-duty truck oil filters are selected, studied and analyzed using the appropriate tests in compliance with SAE (Society of Automobile Engineers) and Boltzmann Theory. The operational efficiency is examined and the reliability of the filter system is assessed systematically by obtaining the filtration performance characteristics such as separation efficiency, filtration performance, discharge, pressure drop etc.

The overall operational efficiency of the oil filters are estimated for diverse contamination modes by:

i. Selection and disassembly oil filter to obtained porous media

ii. Filter media identification by labeling A, B and C

iii. Particulate size analysis of contaminant (test dust)

iv. Computing the flow characteristics, such as pressure drop, discharge etc. of filter element

v. Estimation of filtration parameters, such as separation efficiency, filtration performance etc. using test dust

vi. Simulation of diffusive flow characteristics across porous media using Boltzmann Theory

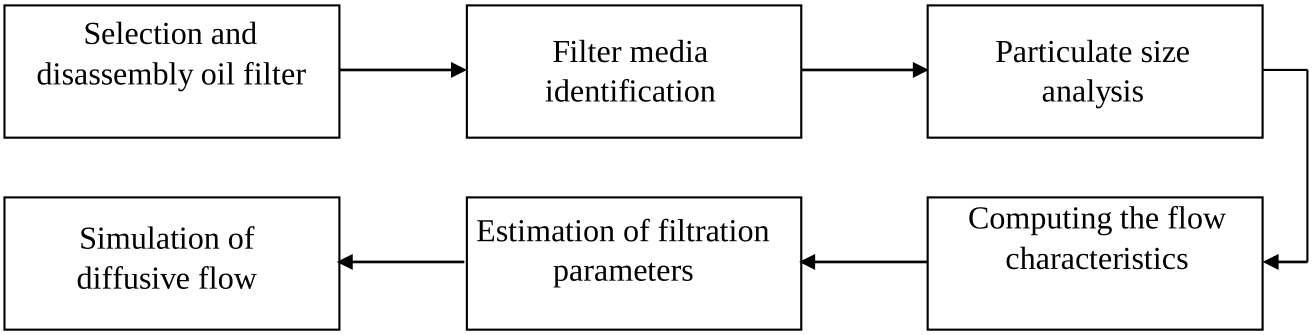

Figure 1.1: *Block Flow Diagram of Approach to Study*

1.2 RESEARCH GAP

Knowledge Gap

Over the years, many research teams have worked on developing equations describing the pressure drop associated with fluid flow through fibrous or porous filter media. Examples of influencing variables in flow through porous media are, for example, average fluid velocity, specific permeability, dynamic viscosity, and thickness (in flow direction) of the bed of porous material. In a study involving flow of air through a porous aluminum layer, [26] showed that pressure drop over the porous layer (the pressure gradient) is proportional to a cubic function of fluid speed (seepage velocity). The cubic equation was in much better agreement with experimental pressure gradient values than the earlier (Forchheimer -extended Darcy) quadratic equation. In addition, the cubic equation was accurate up to a fluid velocity of 19.26 m/s [27].

In another study by [28] involving compressed and uncompressed open-cell aluminum foam samples tested in a wind-tunnel setting, it was found that the pressure drop followed a quadratic equation with respect to the seepage velocity. In that study, however, the highest seepage velocity in the experiments was 2.73 m/s, implying that the quadratic correlation equation could be adequate at low seepage velocities. Studies involving model equation building for fibrous cartridge oil filters appear to be infrequent compared to studies involving air filters [29-32].

In a paper by [33] an equation was developed for the pressure drop (and the friction factor) for fluid flow through fibrous material beds. However, this equation was developed for clean filters, which restricts its usage in filter condition monitoring. An example of a diagnostic system for hydraulic filters in industrial use (in connection with a system of servo hydraulic actuators) [32-35]. The software developed in the study was used for predicting the service life of the hydraulic filter based on the evolution of the pressure difference over the filter. A cost-effective way of estimating the flow rate (using down-stream pressure measurement instead of flow meters) was presented and thus the effect of flow rate on the pressure difference was taken into account. However, the work did not take the effect of changing viscosity (temperature) on the pressure difference over the filter into account [34-40].

For this study, extensive laboratory experiments have been conducted for observing how the pressure drop over a hydraulic depth filter develops as the filter is being subjected to a stream of particle-contaminated oil at different flow and fluid conditions. The different conditions included the oil gravimetric contamination level, the oil flow rate, and the oil viscosity, which was varied by varying the oil temperature. From these experiments, a mathematical correlation model has been derived in this work for describing the evolution of the pressure drop based on the aforementioned flow and fluid conditions. The modeling process also included an investigation on how the apparent dirt holding capacity of the filter seems to vary at the different flow and fluid conditions [40-45].

Due to the lack of mandatory standardized testing, some truck owners have had catastrophic engine damage from using an inferior oil filter. The idea for this research came through the desire to find the best designed and manufactured truck oil filters. An analysis protocol was developed and applied to the sample of 5 oil filters in order to accurately determine and compare filter design characteristics and its operational efficiency by integrating Boltzmann Theory [46].

The fluid-particle flow plays an important role in experiment and industrial process of particle filtration, it is essential to understand the phenomenon of particle transport in fluid flow and the relative physical problems. Because the cost of experiments can be excessive and some information cannot be easy to obtain experimentally, numerical simulation of fluid-particle flow provides a promising way to deal with this kind of issues. In recent years, researchers of this field have developed fluid-particle flow models such as one-way coupling, two-way coupling and four-way coupling

[47]. One-way coupling means the fluid phase and solid phase are computed separately, only considering the drag force acting on the particles. Two-way coupling means that the back effect of solid phase on the fluid phase is taken into account. Four-way coupling considers the fluid-particle and particle-particle interactions [48].

The fluid-particle flow models have gradually popularized from one-way coupling to two-way coupling and four-way coupling. In terms of volume fraction of particles Φp. For a low value of $\Phi p \leq 10{-}6$, the effect of particle on the fluid can be neglected, thus one-way coupling could be sufficient. In the second regime $10{-}6 < \Phi p \leq 10{-}3$, the mutual interaction between the fluid and particle need to be considered: two-way coupling. As increased in the volume fraction of particle $\Phi p > 10{-}3$, both the fluid-particle interaction and particle-particle interaction should be included, four-way coupling is needed. In this section, different types of numerical models for simulating the particle transport in fluid flow are outlined. It includes the numerical methods for fluid phase and particle phase respectively [49-51].

2. METHODOLOGY

Materials

Filter material samples (filter cartridges) were selected for testing from different heavy-duty trucks, with Gross Vehicle Weight Rating (GVWR) of 65,000pounds (almost 30,000kgs), used in transporting huge weights of cargo at Shell Petroleum Development Company, Port Harcourt, and were marked as A (Mobil 1), B (Deutsch) and C (Penzoil). The oil filter is cut open on a lathe and obtain the porous filter media within on which appropriate tests to determine their operational efficiency. Filter materials data were summarized in the table 1.

Table 1: Manufacturer's Specifications for Filter A

Filter A: Mobil 1 (M1-301)

Cartridge Length	4.250 inches
Cartridge Outside Diameter	3.250 inches
Cartridge Inside Diameter	1.625 inches
Cartridge Pleats	52
Cartridge End Cap Type	Stamped-steel, with bypass valve

Anti-Drainback Valve Type	Nitrile rubber diaphragm
Bypass Valve Type	Spring-loaded steel, nitrile seal
Element Type	Synthetic media, glued seam
Element Length	85 inches
Element Width	4.125 inches
Element Surface Area	351 square inches
Backplate Thickness	0.138 inches
Gasket Type	Nitrile rubber
Hydrostatic Burst Pressure	600 psi
Filtration Efficiency	Unknown

The evaluation was carried out in two stages, with the following courses:

i. Flow characteristics $\Delta p_w = f(Q_w)$ of selected filter materials (cartridges) were made by making five repetitions for each Q_w value.

ii. Efficiency φ_w, filtration accuracy d_{zmax} and flow resistance Δp_w characteristics depending on dirt absorption coefficient k_m of three filter cartridges of each material, A, B and C were made.

Measurement result analysis was performed in the scope of:

i. From each material, A, B and C, one of the sample characteristics were selected in order to compare (on one graph) their initial efficiencies and duration of the initial period, as well as changes in flow resistance depending on dirt absorption coefficient k_m.

ii. On the example of cartridge A, changes in the number of dirt grains in the air behind the filter cartridges in successive measuring intervals and after subsequent test cycles are presented.

iii. On the example of filter cartridge A and C, the particle size distribution of grains in the exhaust air was analyzed after measurement No. 1 and after measurement corresponding to the end of the initial filtration period.

iv. Using the quality factor q, the filtration properties of the tested material samples were assessed.

The test is carried out to determine and compare the filtration parameters including separation efficiency, filtration performance and pressure drop at the filter elements made of different filter media by determining the following filtration characteristics:

a) Filtration performance $d_{zmax} = f(k_m)$;

b) Separation efficiency $\varphi_w = f(k_m)$;

c) Pressure drop $\Delta p_w = f(k_m)$;

d) Flow (aerodynamic) characteristics $\Delta p_w = f(Q_w)$;

Methods

Test on porous filter media

Tests were carried out on a test stand with a Pamas 2132 particle counter with HCB-LD-2A-2000-1 sensor. The particle counter records the number and size of dirt particles in the air Q_w downstream of the filter element from 0.7 to 100 µm at i = 32 intervals by diameter ($d_{zmin} - d_{zmax}$).

The filter element test stand: 1–filter element, 2—dirt chamber, 3—dirt dispenser, 4—rotameter, 5—U-tube manometer, 6—measuring tube, 7—humidity, ambient air temperature and pressure measurement unit, 8—measuring probe, 9—absolute filter, 10—sensor, 11—particle counter, 12—measuring computer, 13—suction fan, 14—rotameter, 15—analytical balance.

For the flow characteristics, the maximum air volume flow rate calculated from the following relationship:

$$Q_{wmax} = A_w \upsilon_{Fw} \times 3600 \ (m^3/h) \tag{1}$$

A RIN 60 type rotameter with a measuring range of 3 to 67 m^3/h and accuracy class of 2.5 was used to measure the air volume flow rate Q_w.

Filtration characteristics of the filter elements: separation efficiency $\varphi_w = f(k_m)$, filtration performance $d_{zmax} = f(k_m)$ and pressure drop $\Delta p_w = f(k_m)$ were determined using a gravimetric method at a constant filtration rate υ_{Fw} = 0.1 m/s.

Dirt mass retained by the tested filter element and the absolute filter in subsequent j cycles after time τ_p (evenly dosing time) to the filter was determined. Dirt concentration at the filter element inlet was s = 0.5 g/m^3. The duration (uniform dirt batching time) was τ_p = 3 min in the initial period (I) and τ_p = 9–12 min in the main period (II) of the filter working time. After each cycle j, the following parameters were determined for the filter element: separation efficiency, filtration performance, pressure drop and dirt absorption coefficient. Dirt mass retained by the filter element and the absolute filter was determined using an analytical balance with a 220-g capacity and a 0.1-mg readability.

During the measuring cycle, the particle counter was activated 60 s before the planned test end to count the number and size of dirt particles in the air downstream of the filter.

Following points were determined after each measuring cycle j:

Pressure drop Δp_{wj} at the filter as a static pressure drop upstream and downstream of the filter based on the measured height Δh_{mj} (after the dirt supply ended) at a U-tube manometer using the following relationship:

$$\Delta p_{wj} = {}^{\Delta h_{mj}}/_{1000} \cdot (\rho_m - \rho_H) \cdot g (Pa) \tag{2}$$

Where ρ_m is the manometric liquid density (kg/m^3), ρ_H is the air density (kg/m^3), g is the gravitational acceleration (m/s^2).

1. Separation efficiency, as a dirt mass product m_{ZFj} retained by the filter and dirt mass m_{Dj} supplied to the filter during the next j cycle based on the following relationship:

$$\varphi_j = {}^{m_{Fj}}\!/_{m_{Dj}} = {}^{m_{Fj}}\!/_{m_{Fj} + m_{Aj}} \times 100\% \tag{3}$$

2. Dirt mass loading k_{mj} of the tested filter medium:

$$k_{mj} = {}^{\sum_{j=1}^{n} m_{Fj}}\!/_{A_w} \ (g/m^2) \tag{4}$$

3. Number of dirt particles N_{zi} in the air stream downstream of the filter (passing through the filter media) in the intervals by diameter ($d_{zimin}$to d_{zimax}).

4. Filtration performance as the largest dirt particle size $d_{zj} = d_{zmax}$ in the air downstream of the filter.

5. Fraction of each dirt particle size in the air downstream of the filter for each cycle:

$$U_{zi} = {}^{N_{zi}}\!/_{N_z} = {}^{N_{zi}}\!/_{\sum_{i=1}^{32} N_{zi}} \times 100\% \tag{5}$$

Where $N_z = \sum_{i=1}^{32} N_{zi}$ – the total number of dirt particles passing through the oil filter (for all measuring intervals) in the test cycle.

Test cycle used in the study involved five counts of dirt particles from the range of 0.7 to 35 µm, divided into 32 intervals by diameter ($d_{zimin}$to d_{zimax}).

In accordance with the method, the following filtration characteristics were determined: separation efficiency $\varphi_w = f(k_m)$, filtration performance $d_{zmax} = f(k_m)$ and pressure drop $\Delta p_w = f(k_m)$ of the filter elements A, B and C.

Three specimens of each filter element with the same filter medium were tested. The flow characteristics $\Delta p_w = f(Q_w)$were determined before the filter element tests using the test contaminant.

2.1 Simulation of Boltzmann Flow through Porous Media

A series of parameters used in the simulations are shown in Table 4.2. Pressure drop is applied between the inlet and outlet of the channel. The flow rate Q can be computed at the outlet of the channel. The term $-k/\mu$ is constant for fixed fluid and porous media. The relationship between Q and $A|\nabla p|$ is obtained using MATLAB and k/μ represents the slope of the line.

Kozeny-Carmann equation is also used to test the MATLAB code. Here we consider the porous media with porosity ϕ, constituted by circular obstacles of diameter d. Varying the number N of obstacle leads different porosity of media in each simulation. For the given fluid and porous media, $\Phi_s^2 \, D_s^2 / 180\mu$ is constant. Therefore relation between Q and $(\phi)^3 / (1-\phi)^2$ is also tested for linearity and hence, validation of the model.

3. RESULT AND DISCUSSION

Results for Flow Characteristics of Filter Media

The parameters of the tested filter media based on the data provided by the manufacturer are shown in Table 2.

Table 2: *Oil filter parameters*

Parameters	**Filter Medium Identification**		
	A (Mobil 1)	**B (Deutsch)**	**C (Penzoil)**
Filter medium	Synthetic media, glued seam	Paper media, glued seam	Paper media, stamped metal seam
Permeability q_p ($m^3/m^2/h$) at 200 Pa	3015	540	685

Parameters	**Filter Medium Identification**		
	A (Mobil 1)	**B (Deutsch)**	**C (Penzoil)**
Basis weight g_m (g/m^2)	121	180	135
Thickness g_z (μm)	610	550	360

$\Delta p_w = f(Q_w)$ of the filter elements were determined at 8 points for the air volume flow rate Q_w = $Q_{wmin} - Q_{wmax}$. The maximum air volume flow rate Q_{wmax} was determined for the maximum filtration rate υ_{Fw}= 0.1 m/s. For the heavy duty truck filters, the maximum filtration rate of the filter paper is between υ_{Fw} = 0.07 to 0.12 m/s. For the filtration rate of (υ_{Fw} = 0.1 m/s), the maximum air volume flow rate calculated and Q_{wmax} = 56 m^3/h.

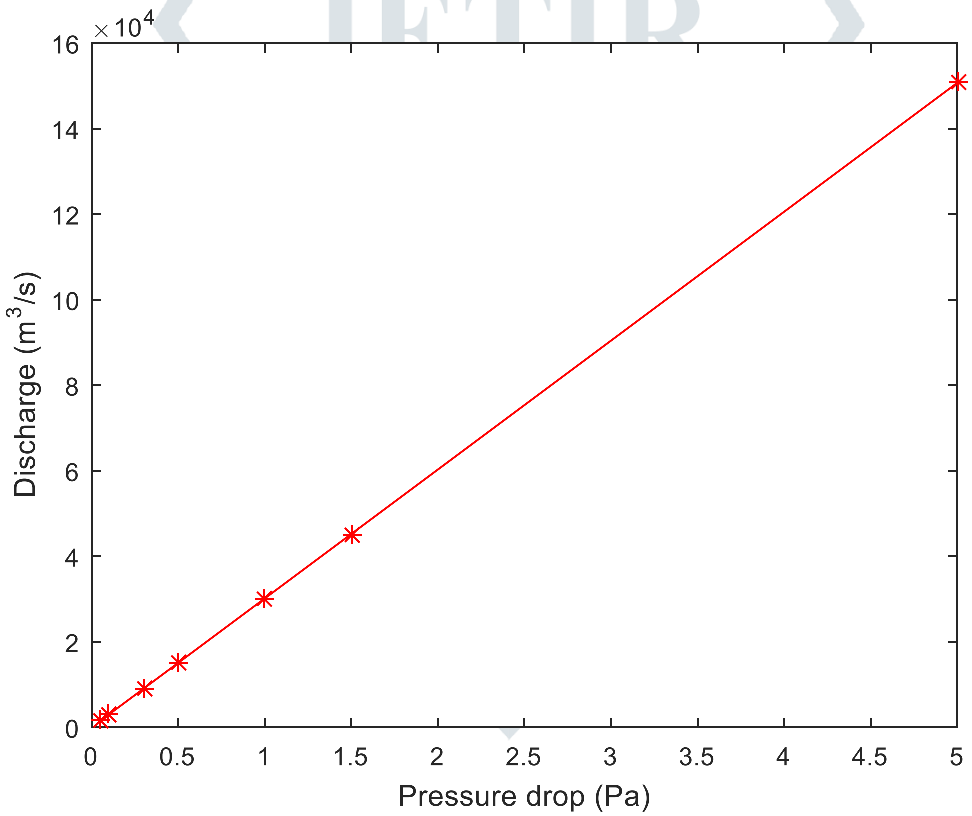

Figure 1: The relationship between discharge Q calculated at the outlet and the pressure gradient for filter A.

In Figure 1, a linear increase in pressure drop Δp_w with an increase in air volume flow rate can be observed, corresponding to the data from the literature.

The filter medium A achieves the lowest pressure drop due to high permeability (838 dm^3/m^2/s), significantly higher than observed for other filter media. The pressure drop at the other filter media (B and C) is between 370 and 410 Pa.

The significantly higher pressure drop at the filter medium for other filter media is due to a very low permeability of the filter bed.

There were observable differences in the values of the initial filtration efficiency (for dust mass loading from 0 to 70 g/m^2) for three filter cartridges). This had a direct impact on the effectiveness of the inertia and direct hooking mechanism, which are decisive in depth filtration in the bed. In particular, it was assumed that the filter material structure and its thickness in each filter cartridge is the same. It was also assumed that the active surface area of the cartridges is the same. With the same value of the air stream Q during the tests, the filtration speed υ_{Fw} should also be the same.

Results of Separation Efficiency Test

Separation efficiency φ_w, filtration performance d_{zmax} and pressure drop Δp_w of one out of three filter element A, B and C specimens were used in the analysis. The characteristics of three filter elements A, B and C with different filter media have a similar form and significantly different values.

With an increase in dust mass retained by the filter layer (increase in k_m factor), separation efficiency, filtration performance and pressure drop of the filter elements A, B and C increase, however, at a different rate and with different initial values. The characteristics are the result of the dust particles being retained by the fiber surface and filling the voids (pores).

By convention, the operation of the tested filter elements can be divided into two stages. The first (I), initial stage of operation of each filter element lasts until the separation efficiency of φ_w = 99.9% is reached. This stage is characterized by a low initial separation efficiency, filtration performance and pressure drop.

Initial separation efficiencies of the tested filter elements vary. The lowest value (φ_{w0A} = 96.3%) was observed for the filter element made of filter medium A. The filters B and C show higher initial separation efficiency, φ_{w0B} = 98/9%, and φ_{w0C} = 98.2% respectively.

Results for Contaminant Mass Retained

With an increase in dust mass retained by the filtration layer (increase in k_m factor), the separation efficiency of the tested filter elements increases. The required separation efficiency (φ_w = 99.9%—end of stage I) is achieved by the filter elements working in similar conditions (the same dust concentration and air volume flow rate) at different times. Filter element A reaches efficiency of φ_w = 99.9% at the mass loading of dust of k_{mA} = 110.7 g/m^2. For the elements B and C made of different filter media, the first stage is significantly shorter. For the filter element B, stage I ends at the mass loading of dust k_{mB} = 31.9 g/m^2, and for the filter element C, at the mass loading of dust k_{mC} = 48.5 g/m^2.

At the beginning of the filtration process, the maximum size of dust particles downstream of the filter (in the filtered air) may vary. The largest dust particles (d_{zmax} = 28 µm) were observed downstream of the filter element A, and the smallest (d_{zmax} = 7.9 µm), downstream of the filter element C which is strictly correlated with the initial separation efficiency of the filter elements. This results from the higher basis weight and smaller pores of the tested filter media.

With an increase in dust mass retained by the filter bed, the particles accumulate at the surface of the porous structure fibers and at the surface of previously accumulated particles, creating constantly growing and complex dendritic structures (agglomerates), filling the voids between the fibers. The result of changes in the bed structure is an increase in separation efficiency. The size of the dust particles downstream of the filter decreases gradually.

The initial stage of operation of filter element A made of cellulose is several times longer than observed for other filter elements. It significantly affects the durability of the engine. Low separation efficiency and filtration performance in the initial stage (after using a new filter element) results in the presence of large dust particles above 5 µm, significantly affecting the premature wear of engine components, mostly piston, piston rings and cylinder sleeves. The duration of the initial filtration stage may be reduced by using the filter medium with a layer of fibrous membrane. High separation efficiency and filtration performance 99.9% is achieved by the filter elements much earlier than in filters made of standard filter media (cellulose) to eliminate the effect of air impurities on premature wear and durability of the engine.

Results for Particulate Size Analysis

The filtered air contains dust particles with different sizes and in different volumes. A predominant particle size is between 0.7 and 1.1 μm. With an increase in dust particle size d_z in the air downstream of the filter, the number of particles N_p is reduced, indicating the increasing separation efficiency of the tested filter medium. In the last interval, a single dust particle is usually present ($d_z = d_{zmax}$ maximum size) that is used as a measure of filtration performance.

The fraction of particles significantly decreases with an increase in dust particle size and the filtration process duration. The fraction of dust particles d_z = 2 μm for measurement no. 1 is Up1 = 11.6%. For subsequent measurements, the fraction of particles d_z = 2 μm increases and for measurement no. 11 is U_{p11} = 1.5%. A similar change in the share of U_p of dust grains in subsequent measurement intervals in the air behind the filter element occurs for other tested materials A, B and C. There are differences in the values of the U_p shares. The shorter the initial period of filtration, the greater the proportion of grains with dimensions d_z = 0.7–1.1 μm.

Separation Efficiency as a Function of Mass Loading of Contaminant

The accumulation of dust particles on the panel filter fibers changes the filter structure, reduces the surface area of the air stream flow around the fibers. The aerosol flow rate increases with an increase in pressure drop at the filter bed. An increase in pressure drop at the tested filter elements, despite similar testing conditions, differed in rate. The pressure drop of Δp_w = 3 kPa is achieved by the filter elements after retaining different masses of dust.

Separation efficiency φ_w and pressure drop Δp_w are computed as a function of the mass loading of dust k_m of the tested filter elements A, B and C. It is determined by the surface filtration during which the dust particles are retained by the filtration layer before reaching the inside of the filter bed. At the point, the filter elements reach the pressure drop of Δp_{maxC} = 3 kPa, they retain and accumulate different masses of dust.

For filter element (A), the initial stage (I) is over 50% of its total service life, and significantly affects the abrasive wear of engine components. For filter elements (C and B), the period is shorter and is 40% and 22% of its total service life, respectively.

In the second (II) stage of the operation of the filter elements B, C, the separation efficiency is maintained at a stable level of φ_w = 99.9%. For the filter element A, a slight and systematic decrease in separation efficiency can be observed. In the last measurement, the separation efficiency was φ_w = 99.7%. It may be due to the accumulation of a significant amount of dust in form of extensive tree-like dendrites.

The dust particles at the top of the dendritic structures are captured and transferred to the outlet side of the filter medium, and captured by the air stream from the engine cylinders. The decrease in the separation efficiency is related with the maximum dust particle size, reaching higher and higher values. For the last measurement, the value was d_{zmaxA} = 16.7 µm. For the remaining filter elements, the maximum dust particle sizes d_{zmax} were stable at a significantly lower level.

Quality Factor of Test Filters

The filtration properties of the tested filter media were evaluated using a quality factor q.

$$q = \frac{-\ln\left(1 - {}^{\varphi_0}/_{100}\right)}{\Delta p}\left(\frac{1}{kPa}\right)$$

Where φ_0 is initial efficiency of the filter bed [%],Δp - pressure drop for nominal air volume flow rate (kPa).

The calculation results indicate that the highest quality factor was observed for specimen B and specimen C: q_B = 15.4 kPa^{-1} and q_C = 15.1 kPa^{-1}, respectively. The specimens reach higher initial values of the separation efficiency: φ_{0wB} = 99.97% and φ_{0wC} = 99.8%, and filtration performance in the initial stage d_{zmaxB} below 15.8 µm and below d_{zmaxC} 7.9 µm, respectively.

A significantly lower value of the quality factor q = 10.6 kPa^{-1} is achieved by specimen A as a result of lower initial separation efficiency φ_{0wA} = 96.3%. The separation efficiency is correlated with the filtration performance. Lower separation efficiency means not only lower mass of dust retained by the filter, but also larger dust particles in the air downstream of the filter, affecting the wear and durability of the internal combustion engine components.

Result of Simulation of Boltzmann Flow through Porous Media

Table 3: *Parameters used in the simulation of the fluid through porous media*

Paramters	**Values**	**Unit**
Channel length, L_x	0.05	m
Channel height, L_y	0.008	m
Porosity, ϕ	0.790	-
Pressure drop, Δp	0.05, 0.1, 0.3	Pa
Fluid kinetic viscosity, ν	10^{-6}	m^2/s
Fluid density, ρ	10^3	kg/m^3
Relaxation time, τ	0.8	-
Lattice spacing, h	5×10^{-5}	M

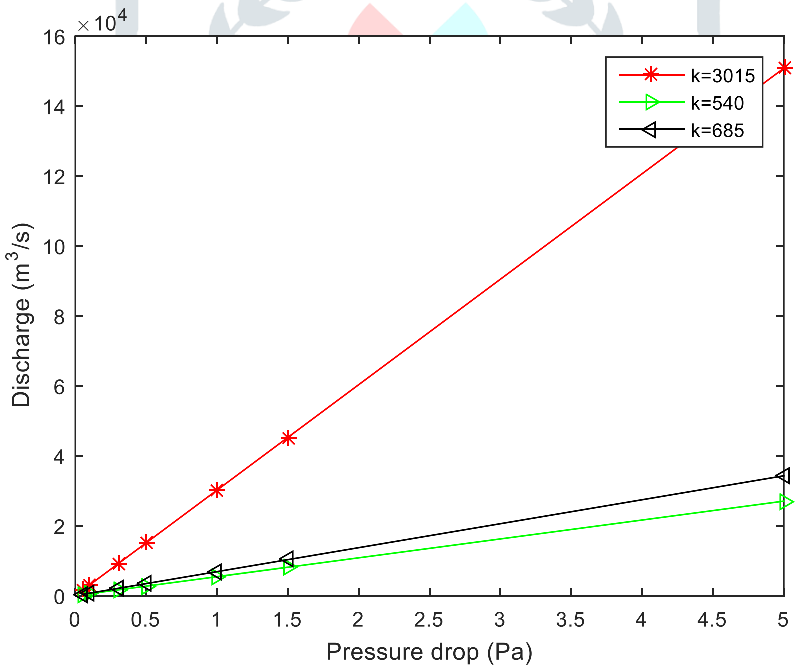

Figure 2: *The relationship between discharge Q calculated at the outlet and the pressure gradient for three filters*

The relationship between discharge Q calculated at the outlet and the pressure gradient Δp for filters A, B and C is represented in the figure above. As a consequence, the relationship of discharge and the product of cross-sectional area and the pressure gradient obtained with MATLAB is tested for linearity.

A filter medium that exhibits a permeability profile i.e. it is not homogeneous with respect to permeability, leads to a fast pressure drop rise at the beginning of filtration. The pressure drop of the studied filter media changes during filtration operation. The impact of porosity depends on permeability through filter media. For high permeability, the higher porosity induces the increase of driving force and accelerates the flow while it decelerates the flow for low permeability by causing stronger viscous drag of the porous medium. Filter A possesses relatively high permeability of 3015 $m^3/m^2/h$ compared to 540 and 685 for B and C respectively, exhibits a linear Darcy flow as depicted by the graphical relationship between the discharge and pressure gradient of filters. Hence filter A shows a relatively high performance and filtration effectiveness compared to B and C, and is more efficient in contamination control in engine of heavy-duty trucks.

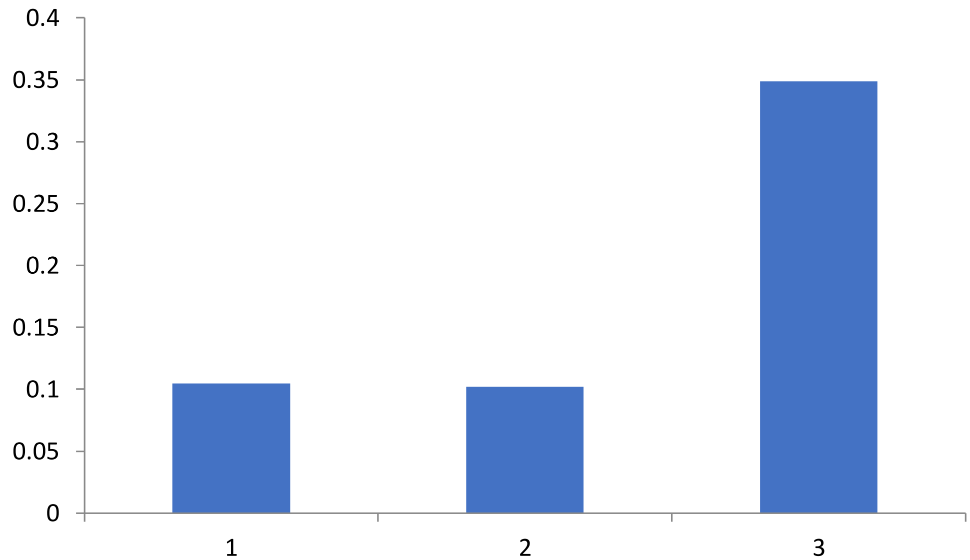

Figure 3: *Filter costs by failure in present value at 18% discount and 1 year service life.*

As shown in Figure 3, considering the relevance of the costs related to the failure presented by the case study analyzed, it is relevant to point out that the organization will incur more than twice the amount needed to repair and maintain each of filters A and B to curtail failure in filter C, as it exhibits the least operational efficiency.

4. CONCLUSION

At the end of our study, we can see and conclude that it is very important to exploit the advanced contamination control in oil filters and maintenance methods. This will allow with accuracy the knowledge and understanding of the behavior of reliability, and the availability of the heavy-duty truck studied, without neglecting the advantage of risk control.

The results show that the filter A has the highest operational efficiency compared to B and C with a long repair time and cost of repair. A maintenance plan was created for the sake of reducing the time to repair and increasing the uptime as a consequence of increasing the reliability and availability of the particular heavy-duty truck by applying the preventive maintenance every systematic time and some remedy of the problems that cause the repair time, this plan also consists a cure for critical failures like redesigning the conditional maintenance for the filter's failure mode.

5. REFERENCE

1. Ansari, V., Goharrizi, A. S., Jafari, S., & Abolpour, B. (2015). Numerical study of solid particles motion and deposition in a filter with regular and irregular arrangement of blocks with using lattice Boltzmann method. *Computers & Fluids*, *108*, 170-178.
2. Baddock, M. C., Zobeck, T. M., Van Pelt, R. S., & Fredrickson, E. L. (2011). Dust emissions from undisturbed and disturbed, crusted playa surfaces: cattle trampling effects. *Aeolian Research*, *3*(1), 31-41.
3. Banihashemi Tehrani, S. M., Moosavi, A., & Sadrhosseini, H. (2016). Filtration of aerosol particles by cylindrical fibers within a parallel and staggered array. *Microsystem Technologies*, *22*(5), 965-977.
4. Bojdo, N., & Filippone, A. (2012). A comparative study of helicopter engine air particle separation technologies.
5. Bojdo, N., & Filippone, A. (2014, September). Effect of desert particulate composition on helicopter engine degradation rate. In *Proceedings of the 40th European Rotorcraft Forum, Southampton, UK* (pp. 2-5).
6. Bojdo, N., & Filippone, A. (2019). A simple model to assess the role of dust composition and size on deposition in rotorcraft engines. *Aerospace*, *6*(4), 44.
7. Brandon, D. J., & Aggarwal, S. K. (2001). A numerical investigation of particle deposition on a square cylinder placed in a channel flow. *Aerosol Science & Technology*, *34*(4), 340-352.
8. Breuer, M., Bernsdorf, J., Zeiser, T., & Durst, F. (2000). Accurate computations of the laminar flow past a square cylinder based on two different methods: lattice-Boltzmann and finite-volume. *International journal of heat and fluid flow*, *21*(2), 186-196.
9. Chan, D., & Stachowiak, G. W. (2004). In Proc. Instn. Mech. Eng.: Part D. *J Automotive Eng.*, *218*, 953-966.
10. Chen, S., Cheung, C. S., Chan, C. K., & Zhu, C. (2002). Numerical simulation of aerosol collection in filters with staggered parallel rectangular fibres. *Computational mechanics*, *28*(2), 152-161.
11. Cui, X., Li, J., Chan, A., & Chapman, D. (2014). Coupled DEM–LBM simulation of internal fluidisation induced by a leaking pipe. *Powder Technology*, *254*, 299-306.
12. Cundall, P. A., & Strack, O. D. (1979). A discrete numerical model for granular assemblies. *geotechnique*, *29*(1), 47-65.
13. Davies, C. N. (1953). The separation of airborne dust and particles. *Proceedings of the Institution of mechanical engineers*, *167*(1b), 185-213.
14. Deng, Y., Fan, J., Zhou, S., Zhou, T., Wu, J., Li, Y., ... & Wu, Y. (2014). Euler force actuation mechanism for siphon valving in compact disk-like microfluidic chips. *Biomicrofluidics*, *8*(2), 024101.
15. Dziubak, T. (2018). Performance characteristics of air intake pleated panel filters for internal combustion engines in a two-stage configuration. *Aerosol Science and Technology*, *52*(11), 1293-1307.
16. Dziubak, T. (2019). Properties of material with nanofiber layer used for filtering the inlet air of internal combustion engines. *Combustion Engines*, *58*.
17. Dziubak, T., & Bąkała, L. (2018). Experimental research of the material filtration characteristics with nanofibers addition. *Journal of KONES*, *25*.
18. Dziubak, T., & Dziubak, S. D. (2020). Experimental study of filtration materials used in the car air intake. *Materials*, *13*(16), 3498.

19. Dziubak, T., & Dziubak, S. D. (2020). Experimental study of filtration materials used in the car air intake. *Materials*, *13*(16), 3498.
20. Dziubak, T., & Szwedkowicz, S. (2015). Operating properties of non-woven fabric panel filters for internal combustion engine inlet air in single and two-stage filtration systems. *Eksploatacja i Niezawodność*, *17*(4).
21. Esnouf, A., Latrille, É., Steyer, J. P., & Helias, A. (2018). Representativeness of environmental impact assessment methods regarding Life Cycle Inventories. *Science of the Total Environment*, *621*, 1264-1271.
22. Feng, J. Y., & Zhang, J. (2014). The Property of Automobile Engine Oil Filtration Material and the Development of New Filter. *Journal of Engineered Fibers and Fabrics*, *9*(3), 155892501400900316.
23. Feng, Y. T., Han, K., & Owen, D. R. J. (2007). Coupled lattice Boltzmann method and discrete element modelling of particle transport in turbulent fluid flows: Computational issues. *International Journal for Numerical Methods in Engineering*, *72*(9), 1111-1134.
24. Feng, Z. G., & Michaelides, E. E. (2004). The immersed boundary-lattice Boltzmann method for solving fluid–particles interaction problems. *Journal of computational physics*, *195*(2), 602-628.
25. Feng, Z. G., & Michaelides, E. E. (2004). The immersed boundary-lattice Boltzmann method for solving fluid–particles interaction problems. *Journal of computational physics*, *195*(2), 602-628.
26. Fitch, J. (2002). Clean oil reduces engine fuel consumption. *Practicing Oil Analysis Magazine*, 11-12.
27. Haider, A. H., & Kang, S. IK (2015). A Comprehensive Review Summarizing the Effect of Electrospinning Parameters and Potential Applications of Nanofibers in Biomedical and Biotechnology. *Arabian Journal of Chemistry*, 1-24.
28. Hakobyan, N. A. (2015). Introduction to Basics of Submicron Aerosol Particles Filtration Theory via Ultrafine Fiber Media. *Armenian Journal of Physics*, *8*(3).
29. Hosseini, S. A., & Tafreshi, H. V. (2010). Modeling particle filtration in disordered 2-D domains: A comparison with cell models. *Separation and Purification Technology*, *74*(2), 160-169.
30. Hosseini, S. A., & Tafreshi, H. V. (2011). On the importance of fibers' cross-sectional shape for air filters operating in the slip flow regime. *Powder technology*, *212*(3), 425-431.
31. Howard, K. (2014). Advanced engine oils to improve the performance of modern internal combustion engines. In *Alternative fuels and advanced vehicle technologies for improved environmental performance* (pp. 138-164). Woodhead Publishing.
32. Huang, H., Wang, K., & Zhao, H. (2016). Numerical study of pressure drop and diffusional collection efficiency of several typical noncircular fibers in filtration. *Powder Technology*, *292*, 232-241.
33. Huertas Cardozo, J. I., & Prato Sánchez, D. F. (2019). An experimental and numerical study of air pollution near unpaved roads. *Air Quality, Atmosphere & Health*, *12*(4), 471-489.
34. Israel, R., & Rosner, D. E. (1982). Use of a generalized Stokes number to determine the aerodynamic capture efficiency of non-Stokesian particles from a compressible gas flow. *Aerosol Science and Technology*, *2*(1), 45-51.
35. Izard, E. (2014). *Modélisation numérique des écoulements granulaires denses immergés dans un fluide* (Doctoral dissertation).
36. Kordas, P. (2006). The influence of the combustion engine work conditions on the cylinder wear in the stand test researches. *Eksploat. I Niezawodn. Maint. Reliab*, *4*, 11-15.
37. Koszałka, G., & Suchecki, A. (2013). Changes in blow-by and compression pressure of a diesel engine during a bench durability test. *Combustion Engines*, *52*.
38. Koszałka, G., & Suchecki, A. (2015). Changes in performance and wear of small diesel engine during durability test. *Combustion Engines*, *54*(3), 34-40.
39. Kristanto, D., & Awang, M. (2002). The Application of Lattice Gas Automata to Study Fluid Flow in Porous Media.
40. Lee, K. W., & Liu, B. Y. H. (1982). Theoretical study of aerosol filtration by fibrous filters. *Aerosol science and technology*, *1*(2), 147-161.
41. Leili, M., Naddafi, K., Nabizadeh, R., Yunesian, M., & Mesdaghinia, A. (2008). The study of TSP and PM10 concentration and their heavy metal content in central area of Tehran, Iran. *Air Quality, Atmosphere & Health*, *1*(3), 159-166.
42. Leonardi, A., Wittel, F. K., Mendoza, M., & Herrmann, H. J. (2014). Coupled DEM-LBM method for the free-surface simulation of heterogeneous suspensions. *Computational Particle Mechanics*, *1*(1), 3-13.

43. Lim, C. T. (2017). Nanofiber technology: current status and emerging developments. *Progress in polymer science*, *70*, 1-17.
44. Lin, K. C., Tao, H., & Lee, K. W. (2014). An early stage of aerosol particle transport in flows past periodic arrays of clear staggered obstructions: A computational study. *Aerosol Science and Technology*, *48*(12), 1299-1307.
45. Liu, J., Pui, D. Y., & Wang, J. (2011). Removal of airborne nanoparticles by membrane coated filters. *Science of the total environment*, *409*(22), 4868-4874.
46. Liu, X., Shen, H., & Nie, X. (2019). Study on the filtration performance of the baghouse filters for ultra-low emission as a function of filter pore size and fiber diameter. *International Journal of Environmental research and public health*, *16*(2), 247.
47. Mays, D. C. (2010). Contrasting clogging in granular media filters, soils, and dead-end membranes. *Journal of environmental engineering*, *136*(5), 475-480.
48. Musthafa, M. M. (2016). Synthetic lubrication oil influences on performance and emission characteristic of coated diesel engine fuelled by biodiesel blends. *Applied Thermal Engineering*, *96*, 607-612.
49. Panko, J., Kreider, M., & Unice, K. (2018). Review of tire wear emissions: a review of tire emission measurement studies: identification of gaps and future needs. *Non-exhaust emissions*, 147-160.
50. Patankar, S. V. (2018). *Numerical heat transfer and fluid flow*. CRC press.
51. Payen, J., Vroman, P., Lewandowski, M., Perwuelz, A., Calle-Chazelet, S., & Thomas, D. (2012). Influence of fiber diameter, fiber combinations and solid volume fraction on air filtration properties in nonwovens. *Textile Research Journal*, *82*(19), 1948-1959.